crystals

MDPI

Article

Influence of the Substituted Ethylenediamine Ligand on the Structure and Properties of $[Cu(diamine)_2Zn(NCS)_4]$·Solv. Compounds

Natalia Tereba [1,*], Tadeusz M. Muzioł [1], Robert Podgajny [2] and Grzegorz Wrzeszcz [1,*]

[1] Faculty of Chemistry, Nicolaus Copernicus University in Toruń, Gagarina 7, 87-100 Toruń, Poland; tmuziol@umk.pl

[2] Faculty of Chemistry, Jagiellonian University, Gronostajowa 2, 30-387 Kraków, Poland; robert.podgajny@uj.edu.pl

* Correspondence: natalia.tereba@wp.pl (N.T.); wrzeszcz@umk.pl (G.W.)

Received: 31 October 2019; Accepted: 26 November 2019; Published: 29 November 2019

Abstract: In this paper, three new heterometallic compounds were described and compared with the molecular formula $[Cu(pn)_2Zn(NCS)_4]$ (**1**), $[Cu(N,N\text{-}Me_2\text{-}en)_2Zn(NCS)_4]$ (**2**), $[Cu(N\text{-}Me\text{-}en)_2Zn(NCS)_4]\cdot\frac{1}{2}H_2O$ (**3**) where pn = 1,2−diaminopropane, *N*,*N*-Me$_2$-en = *N*,*N*-dimethylethylenediamine and *N*-Me-en = *N*-methylethylenediamine, respectively. The compounds mentioned above were characterized by elemental analysis, infrared (IR), electronic, electron paramagnetic resonance (EPR) spectra, and magnetic studies. Crystal structures for **1** and **2** were determined by X-ray analysis. Copper(II) in these complexes adopts 4 + 2 coordination with two elongated (in **2** very long and considered as semi-coordination) Cu-S bonds. The Cu-N and Cu-S bond lengths depend on substituent position affecting steric hindrance and hence a topology of the chain. Both chains form different zigzag patterns characterized by one or two Cu-Zn distance values. Weak magnetic interaction is observed, ferromagnetic in the case of **1** and antiferromagnetic in the case of **2**, due to diversity of the above structural features.

Keywords: heterometallic complexes; single-crystal X-ray analysis; solvatomorphism; magnetism; EPR; spectroscopy; thiocyanate; bridges; copper(II); zinc(II)

1. Introduction

In recent decades, coordination polymers (CPs) have engaged attention owing to their interesting structural topology features and resulting properties. The key towards the diversity of CPs is the design of underlying topology and directionality, which is realized by a judicious choice of metal centers and ligands. The thiocyanato ligands are often considered because of their ambidentate nature [1–4] and ability to efficiently mediate super-exchange magnetic interaction between paramagnetic metal centers [5]. The thiocyanato-N/S-metalates in reaction with various cationic tectons form numerous zero- [6,7], one- [8,9], two- [10,11], and three-dimensional [4,12] thiocyanato bridged compounds, which manifest interesting structural, physicochemical properties, as well as sometimes potential applications.

The properties of thiocyanato-N/S-metalates very frequently also lead to one-dimensional chain topologies involving pairs of paramagnetic 3d-3d′ [13,14] and 3d-4d metal ions [15], though the diamagnetic centers are in use [12,16]. The first structurally characterized (X-ray single crystal analysis) compound with $[Cr(NCS)_6]^{3-}$ unit in combination with Ni(II), $[Ni(en)_3]_n[\{Ni(en)_2Cr(NCS)_6\}_{2n}]$ [8] is composed of isolated cationic unit $[Ni(en)_3]^{2+}$ and polymeric one-dimensional anion $[\{(SCN)Cr(NCS)_5Ni(en)_2\}_n]^{n-}$. The thiocyanato bridges combine alternately the Cr and Ni centers giving the zigzag pattern. In this compound, moderately strong antiferromagnetic interactions between metal centers in the chain were found and

explained by the structural aspects connected to N,S-thiocyanato bridged entity being in *cis* positions at both metallic centers. The another compound exploiting bridging ability of thiocyanate with diamine as a co-ligand, $[Cu(en)_2Cr(NCS)_4(NH_3)_2][Cr(NCS)_4(NH_3)_2]\cdot 6dmf$, consists of cationic zigzag chains $-NCS-Cu(en)_2-SCN-Cr(NCS)_2(NH_3)_2-$, isolated $[Cr(NCS)_4(NH_3)_2]^-$ unit and solvent molecules [13]. A very low coupling constant ($J = -0.02$ cm^{-1}) was found using the model that assumes antiferromagnetic interactions between metal centers through nearly an orthogonal thiocyanato bridge. The other diamines were also used as blocking ligands to support 1D chain topologies. For example, in the one-dimensional compound $[Cu(oxpn)Ni(\mu\text{-}NCS)(NCS)(tmen)]_n$, (oxpn = *N*,*N*′-bis(3-aminopropyl)oxamidate and tmen = *N*,*N*,*N*′,*N*′-tetramethylethylenediamine), the interactions through bridging thiocyanate ions are negligible, while antiferromagnetic interactions between the chains are transmitted by the hydrogen bonds [17].

In the recent papers of Pryma et al. [18] and Wrzeszcz et al. [19,20], the new compounds with the same $[Cu(en)_2Zn(NCS)_4]$ (en = ethylenediamine) zigzag unit were reported. Among these solvatomorphic compounds, there are different chain types, bond distances and angles, physical properties (density), solvent molecules, etc., depending on the synthesis conditions. As a continuation of our work on this topic, in this paper, three complexes obtained with different diamine ligands were described and compared but with the same metal centers as previously reported [18–20]. Moreover, for obtained compounds, magnetic data were discussed, and attempts were made to determine the impact of the used diamine ligands on the structure.

2. Materials and Methods

2.1. Materials

All reagents used in the synthesis were of analytical grade and used without further purification. Diamine ligands were purchased from Sigma-Aldrich (Darmstadt, Germany), other reagents from POCH (Gliwice, Poland).

2.2. Synthesis of [Cu(diamine)$_2$Zn(NCS)$_4$]

(**1**) 242 mg $Cu(NO_3)_2\cdot 3H_2O$ (1 mmol) (Chempur, Piekary Śląskie, Poland) was dissolved in 16 cm^3 of water. Then, constantly stirring, 0.18 cm^3 99% (2.1 mmol) of 1,2−diaminopropane (pn) (Sigma-Aldrich, Darmstadt, Germany) was slowly added. An inky solution was obtained. In addition, 326 mg of NaNCS (4 mmol) (POCH, Gliwice, Poland) was dissolved in 12 cm^3 of water and added to the solution of 298 mg $Zn(NO_3)_2\cdot 6H_2O$ (1 mmol) (POCH, Gliwice, Poland) in 12 cm^3 of water. Both solutions were combined with vigorous stirring. The clear solution was left to evaporate in the air for two weeks. The violet crystals of $[Cu(pn)_2Zn(NCS)_4]$ (**1**) suitable for diffraction experiments were obtained. The crystals were filtered off and washed with a small quantity of ethanol (POCH, Gliwice, Poland). Total yield: 342 mg (67%). Anal. Found: C, 23.48; H, 3.54; N, 22.00%. Calc. C, 23.57; H, 3.96; N, 21.99%. VIS (cm^{-1}): 18040 d-d (Cu(II)). IR (cm^{-1}): ν(NH) 3302 s, 3223 s, 3119 m, ν(CH) 2967 m, 2924 m, ν(CN) 2085 vs, 2047 vs, δ(NH_2) 1571 s, δ(CH_2) 1459 m, ν(CN) 1052 s, 1012 s, ν(CC) 933 m, ν(CS) 831 m, $\delta_{rocking}(NH_2)$ 674 s, δ(NCS) 477 s, δ(NCuN) and ν(ZnN) 271 s,vbr, δ(ZnNC) 155 s.

(**2**) This complex was obtained in a similar way to **1**, except for the use of *N*,*N*-dimethylethylenediamine (*N*,*N*-Me_2-en) (Sigma-Aldrich, Darmstadt, Germany) instead of pn. The dark violet crystals of $[Cu(N,N\text{-}Me_2\text{-}en)_2Zn(NCS)_4]$ (**2**) suitable for diffraction experiments were obtained. Total yield: 268.7 mg (52%). Anal. Found: C, 26.96; H, 4.61; N, 20.40%. Calc. C, 26.81; H, 4.50; N, 20.84%. VIS (cm^{-1}): 17720 d-d (Cu(II)). IR (cm^{-1}): ν(NH) 3204s, 3129 s, ν(CH) 2983 w, ν(CN) 2133 sh, 2097 vs,br, δ(NH_2) 1581 s, δ(CH_2) 1459 s, ν(CN) 1056 s, 1024 m, ν(CC) 995 s, ν(CS) 820 m, $\delta_{rocking}(NH_2)$ 649 m, δ(NCS) 472 s, δ(NCuN) and ν(ZnN) 278 s, 253 sh, δ(ZnNC) 163 s.

(**3**) This complex was obtained in a similar way to **1**, except for the use of *N*-methylethylenediamine (*N*-Me-en) (Sigma-Aldrich, Darmstadt, Germany) instead of pn. Despite a big effort and experiments performed also in H-tubes, the violet crystals of $[Cu(N\text{-}Me\text{-}en)_2Zn(NCS)_4]\cdot\frac{1}{2}H_2O$ (**3**) unsuitable for diffraction experiments were obtained. The crystals were filtered off and washed with a small quantity

of ethanol. Total yield: 186.7 mg (36%). Anal. Found: C, 23.13; H, 4.06; N, 21.57; H_2O, 1.72%. Calc. C, 23.16; H, 4.08; N, 21.61; H_2O, 1.74%. VIS (cm^{-1}): 17760 d-d (Cu(II)). IR (cm^{-1}): ν(OH) 3456 m, br, ν(NH) 3204 s, 3125 m, ν(CH) 2945 m, ν(CN) 2133 sh, 2092 vs, br, δ(NH_2) 1577 s, δ(CH_2) 1453 m, ν(CN) 1058 s, ν(CC) 977 s, ν(CS) 823 m, $\delta_{rocking}$(NH_2) 657 m, δ(NCS) 472 s, δ(NCuN) and ν(ZnN) 276 s,br, δ(ZnNC) 161 s. Considering the above, some results related to compound **3** have been shown in Supplementary Materials).

Unexpectedly, the use of 1,3-diaminopropane (tn) (Sigma-Aldrich, Darmstadt, Germany) instead of pn, leads to the formation of the blue crystals of known monometallic two-dimensional [Cu(tn)$(NCS)_2$] complex [21,22]. Despite many attempts, the heterometallic [$Cu(tn)_2Zn(NCS)_4$]·Solv. compound has not been synthesized.

2.3. Physical Measurements

Elemental analysis was performed on a Vario Macro CHN Analyzer (Elementar Analysensysteme GmbH, Langenselbold, Germany). Water content was determined on an SDT 2600 (TA Instruments, New Castle, USA) by simultaneous thermogravimetric analysis (TGA) and differential thermal analysis (DTA) in air atmosphere. Infrared spectra (IR) were recorded on a Vertex 70 v Spectrometer (Bruker Optik GmbH, Ettlingen, Germany) in the range 4000–100 cm^{-1}. Reflectance spectra were recorded in MgO on the SPECORD M40 Spectrophotometer (Carl Zeiss, Jena, DDR) in the range 30,000–12,000 cm^{-1}. Electron Paramagnetic Resonance (EPR) spectra of powdered samples were recorded at room temperature with an EPR SE/X 2541 M spectrometer (Radiopan, Poznań, Poland) in X band (ca. 9.33 GHz) with 100 kHz modulation. The microwave frequency was monitored with a frequency meter. The magnetic field was measured with an automatic NMR-type magnetometer. Magnetic measurements in the temperature range 1.8–300 K were performed using a SQUID MPMS-3 magnetometer (Quantum Design, San Diego, USA) at the magnetic field of 0.1 T. The data were corrected for the sample holder, diamagnetism using the Pascal's constants [23] (–278 and $-302 \cdot 10^{-6}$ cm^3 mol^{-1}, for compounds **1** and **2**, respectively) and temperature independent paramagnetism [24]. The effective magnetic moment was calculated from the equation: $\mu_{eff} = 2.828\ (\chi_M{}^{corr} \cdot T)^{1/2}$. Magnetization versus magnetic field measurements were carried out at 1.8 K in the magnetic field range 0–7 Tesla.

2.4. Structural Analysis

Diffraction data were collected at BL14.2 beamline (HZB, Berlin, BESSY II synchrotron) at 100 K for [Cu$(pn)_2$][Zn$(NCS)_4$] (**1**) and on Oxford Sapphire with CCD area detector [25] at room temperature for [Cu(*N*,*N*-Me_2en$)_2$Zn$(NCS)_4$] (**2**). The data were processed using XDS for **1** and CrysAlis for **2**. Subsequently, these data were reprocessed with CrysAlis to apply the numerical absorption correction (RED171 package of programs, Oxford Diffraction, 2000 [25]). Both structures were solved by direct methods and refined by full-matrix least-squares techniques on F^2 with a SHELXL program [26] with anisotropic thermal displacement parameters for all heavy atoms. Positions of hydrogen atoms attached to carbon atoms were assigned at calculated positions, whereas positions of hydrogen atoms attached to nitrogen atoms were found from difference electron density maps. All hydrogen atoms were refined with isotropic thermal displacement parameters fixed to a value of 20% or 50% higher than those of the corresponding C or N atoms. In **1,** we found two sets for positionally disordered CH_2 and CH groups from 1,2-diaminopropane ligands. The refinement showed that they are populated 0.6:0.4 and 0.7:0.3 for Cu2 and Cu3 moieties, respectively. In **2,** positional disorder for CH_2 and CH_3 groups is also observed with two sets refined with final occupancies 0.62 and 0.38. In **2,** two geometrical restraints (DFIX) were applied for C5-H5C/D bonds. Additionally, an extinction coefficient was also refined showing value of 0.0264. All figures were prepared in DIAMOND [27] and ORTEP-3 [28,29]. The details concerning the data collection and refinement processes of the compound reported in this paper are presented in Table 1.

Table 1. Crystal data and structure refinement for **1** and **2**.

Parameters	1	2
Empirical formula	$C_{10}H_{20}CuN_8S_4Zn$	$C_{12}H_{24}CuN_8S_4Zn$
Formula weight	509.49	537.54
Temperature [K]	100(2)	293(2)
Wavelength [Å]	0.7999	0.71073
Space group	Triclinic, *P –1*	Monoclinic, *P 2$_1$/m*
Unit cell dimensions [Å] and [°]	*a* = 8.6630(6) α = 97.190(7) *b* = 8.9219(7) β = 97.164(6) *c* = 13.5420(11) γ = 98.772(6)	*a* = 8.2626(3) α = 90 *b* = 16.4982(6) β = 95.317(4) *c* = 8.2895(3) γ = 90
Volume [Å^3]	1015.19(14)	1125.14(7)
Z, Calculated density [Mg/m^3]	2, 1.667	2, 1.587
Absorption coefficient [mm^{-1}]	2.650	2.396
F(000)	518	550
Crystal size [mm]	0.205 × 0.180 × 0.080	0.500 × 0.360 × 0.090
Theta range for data collection [°]	2.924–32.209	2.468–26.370
Limiting indices	−11 ≤ h ≤ 11 −11 ≤ k ≤ 11 −18 ≤ l ≤18	−10 ≤ h ≤ 9 −20 ≤ k ≤ 20 −10 ≤ l ≤ 10
Reflections collected / unique	16727/4431 [*R*(int) = 0.0298]	6640 / 2383 [*R*(int) = 0.0291]
Completeness to theta	28.681° 89.5%	25.242° 99.9%
Absorption correction	Numerical	Numerical
Max. and min. transmission	0.816 and 0.613	0.813 and 0.380
Refinement method	Full-matrix least-squares on F^2	Full-matrix least-squares on F^2
Data/restraints/parameters	4431 / 0 / 247	2383 / 2 / 164
Goodness-of-fit on F^2	1.056	1.068
Final R indices [$I > 2$sigma(I)]	$R1^a$ = 0.0381, $wR2^b$ = 0.1000	$R1^a$ = 0.0345, $wR2^b$ = 0.0917
R indices (all data)	$R1^a$ = 0.0413, $wR2^b$ = 0.1018	$R1^a$ = 0.0417, $wR2^b$ = 0.0946
Extinction coefficient	N/a	0.0264(19)
Largest diff. peak and hole [eÅ^{-3}]	1.039 and −0.871	0.631 and −0.546

[a] $R1 = \Sigma||F_0|-|F_c||/\Sigma|F_0|$, [b] $wR2 = [\Sigma w(F_0^2 - F_c^2)^2/\Sigma(w(F_0^2)^2)]^{1/2}$.

CCDC **1946058** and **1946055** contain the supplementary crystallographic data for **1** and **2**, respectively. These data can be obtained free of charge from The Cambridge Crystallographic Data Centre [30].

3. Results and Discussion

3.1. General and Spectroscopic Characterization of 1 and 2

3.1.1. General Characterization

Compounds **1** and **2** were synthesized by mixing stochiometric amounts of in situ prepared aqueous solutions of the appropriate bis(diamine)copper(II) congeners and tetra(thiocyanato-*N*)zincate(II) complexes. Elemental analyses confirmed the composition of the complexes investigated. All obtained compounds are air stable, water soluble, and could be easily recrystallized giving violet or dark violet crystals.

3.1.2. Electronic Spectra

Compounds **1** and 2 include thiocyanate groups and pn or *N*,*N*-Me_2-en as ligands, respectively. Electronic spectra of the described compounds for solid samples show a wide, asymmetric band at 18,040, 17,720 cm^{-1} for **1** and **2**, respectively, which was assigned to the $^2B_{1g} \rightarrow {}^2B_{2g}, {}^2E_g$ spin allowed d–d transitions in copper(II) ions [31]. A shoulder of the main band occurring at lower wavenumbers (*ca.* 14,000 cm^{-1}) may be attributed to the $^2B_{1g} \rightarrow {}^2A_{1g}$ d–d transitions [31]. The Jahn–Teller effect is responsible for this asymmetry. Such effect has been previously observed for diversity of copper(II) thiocyanato complexes with identical CuN_4S_2 chromophore, monometallic e.g., $Cu(NH_3)_4(SCN)_2$ [32] and $Cu(en)_2(SCN)_2$ [33], as well as heterobimetallic [20,34–39].

3.1.3. Infrared Spectra

The infrared spectra of **1** and **2** are quite similar to each other and to that of $[Cu(en)_2Zn(NCS)_4]\cdot H_2O$ [19]. They show the characteristic absorptions due to thiocyanato ligands as follows: an intense bands at 2085, 2047 (**1**), 2133sh, 2097 cm^{-1} (**2**), a medium band at 831 (**1**), 820 cm^{-1} (**2**), and strong band at 477 (**1**), 472 cm^{-1} (**2**) due to vibrations of the CN, CS, and deformation of NCS groups, respectively [13,14,40]. The broad and split band in the region 2150–2000 cm^{-1} corresponds to the presence of bridging and N-bonded thiocyanate groups. As pointed out in the literature, the shoulder at the higher frequency (ca. and above 2100 cm^{-1}) can be assigned to bridging ions [40]. The expected low intensity new ν_{CS} bands are masked by strong and medium bands from rocking NH_2. Bands coming from pn molecules were found at: 3302, 3223 and 3119 ν(NH), 2967, 2922 ν(CH), 1571 δ(NH_2), 1459 δ(CH_2), 1052, 1012 ν(CN), 674 $\delta_{rocking}(NH_2)$, and 933 cm^{-1} ν(CC). Bands coming from *N*,*N*-Me_2-en molecules were found at: 3204 and 3129 ν(NH), 2983 ν(CH), 1581 δ(NH_2), 1459 δ(CH_2), 1056, 1024 ν(CN), 649 $\delta_{rocking}(NH_2)$, and 995 cm^{-1} ν(CC). Other bands given in the Experimental section, especially those associated with vibrations and deformations of metal-ligand skeleton, were assigned according to the literature data for $[Cu(diamine)_2]^{2+}$ [41] and $[Zn(NCS)_4]^{2-}$ [42]. The data of elemental analysis confirmed theoretically established formula in each case.

3.2. Description of the Crystal Structures

3.2.1. Structure of Compound (1)

Compound **1** crystallizes in the triclinic *P –1* space group. In the asymmetric unit of the unit cell, a zinc block with four thiocyanate anions and two halves of copper units was found with only one symmetrically independent molecule of pn in the coordination sphere of each copper ions (Figure 1). In this structure, both copper atoms are positioned at the inversion centers. CH_2 and CH groups in both copper units reveal positional disorder with two populations: 0.6:0.4 and 0.7:0.3 for Cu2 and Cu3, respectively, which is related to both enantiomers of chiral pn ligand (S and R, respectively) coordinated to both copper(II) ions from the asymmetric unit cell. The selected bond distances and angles are listed in Table 2 and Table S1. Both copper coordination spheres are composed of four nitrogen atoms from two pn molecules and two sulfur atoms from two thiocyanate anions. Both copper(II) ion adopt 4 + 2 coordination with four short Cu–N bonds ranging from 1.993(2) to 2.031(3) Å for Cu2 and from 2.006(3) to 2.017(3) Å for Cu3. Hence, only in the Cu2 block, we observe asymmetry in Cu-N bonds: NH_2 group next to the CH group shows significant shortening of the Cu–N bond. The N–Cu–N angles show values of 84.92(10) and 84.73(13)° inside Cu2 and Cu3 chelate rings, respectively, 95.08(10) and 95.27(13)° for atoms belonging to two different organic ligands and 180.0° for *trans* oriented nitrogen atoms. Both crystallographically independent $[Cu(pn)_2]^{2+}$ moieties are inclined by 30.94(17)°. The coordination sphere is completed by two sulfur atoms from thiocyanato ligands occupying *trans* positions and found at long distances but significantly differing: 2.9718(8) and 3.0432(9) Å for S3 and S4 atoms, respectively. They form S–Cu–N angles ranging from 85.47(8) to 94.53(8)° and from 88.00(8) to 92.00(8)° for S3 and S4 atoms, respectively. Zinc(II) ion was found in a tetrahedral environment with four nitrogen atoms from thiocyanate anions forming the coordination sphere. Zn–N bonds are slightly shorter for non-bridging nitrogen atoms (1.950(3) and

1.965(3) Å), whereas, for both bridging nitrogen atoms, we found 1.969(3) Å. The N–Zn–N angles range from 103.74(13) to 114.19(12)° for angles between bridging and terminal thiocyanato ligands. The angles between the non-bridging ligands (111.90(12)°) as well as between the bridging ligands (105.56(15)°) fall into this broad range. Generally, the $Zn(NCS)_4^{2-}$ unit has geometrical parameters consistent with those normally observed [43]. The detailed analysis of Cu(II) and Zn(II) coordination spheres for **1**, **2**, and comparison with $Cu(en)_2[Cd(SCN)_3]_2$ [4], $\{Cu(en)_2[Ni(en)(NCS)_2(SCN)]_2\}_n$ [10], $[Cu(en)_2Zn(NCS)_4]\cdot H_2O$ [19], $[Cu(en)_2(SCN)_2]$ [44], and $[Cu(en)_2Cd(dca)_2(SCN)_2]_n$ [45] can be found in Supplementary Materials.

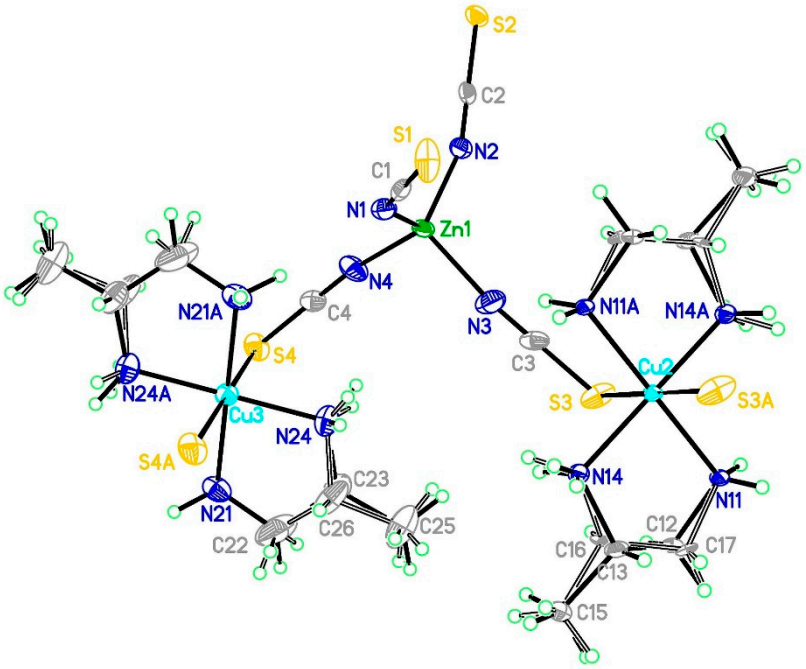

Figure 1. The representative portion of the crystal structure of **1** with the numbering scheme and the thermal ellipsoids at 30% probability. Black bonds correspond to atoms in the main population and grey to the minor one.

Table 2. Selected bonds lengths [Å] for **1**.

Bond	Length	Bond	Length	Bond	Length
Zn1–N2	1.950(3)	Cu2–N14 ^{i}	1.993(2)	Cu3–N24	2.006(3)
Zn1–N1	1.963(3)	Cu2–N14	1.993(2)	Cu3–N24 ^{ii}	2.006(3)
Zn1–N3	1.969(3)	Cu2–N11 ^{i}	2.031(3)	Cu3–N21	2.017(3)
Zn1–N4	1.969(3)	Cu2–N11	2.031(3)	Cu3–N21 ^{ii}	2.017(3)
		Cu2–S3 ^{i}	2.9718(8)	Cu3–S4 ^{ii}	3.0432(9)
		Cu2–S3	2.9718(8)	Cu3–S4	3.0432(9)

^{i} −x+1,−y+1,−z+1; ^{ii} −x,−y+1,−z+2.

In the packing, we observe infinite chains running along the [1 0 −1] direction with alternately arranged copper and zinc ions showing the following repeating motif: … ZnCu2ZnCu3 … (Figures 2 and 3). Copper atoms form the axis of the zigzag, whereas zinc(II) cations were found above and below the axis of the chain propagation. Due to the presence of two crystallographically distinct blocks, there is a variety of intermetallic distances. In the chain, Zn1–Cu3 separation is small (5.0391(5) Å), whereas Zn1–Cu2 distance is much longer (6.3630(6) Å). Hence, Zn–Zn distance across Cu2 atom is 12.726 and across Cu3 atom 10.078 Å. These differences are due to the Zn–S–Cu angle, which, for S3 thiocyanato bridging, Cu2 and Zn1 atoms are much bigger (108.77(2)°) than for S4 anion coupling Cu3 and Zn1 atoms (77.83(2)°). It results in an "irregular" zigzag with one side significantly

extended (Zn1−Cu2−Zn1[1−x, 1−y, 1−z]). It should be noted that a term "irregular" means that two values describe adjacent Cu-Zn distances, whereas "regular" corresponds to only one such value (compare Figure 2 with Figure 5), which is related to the number of independent copper moieties in the asymmetric units. In **1,** the shortest intermetallic distances between paramagnetic copper(II) ions are 7.569, 8.481, and 8.663 Å. The second value corresponds to intrachain separation, whereas other distances describe separations between copper(II) ions in adjacent chains translated along *a* and *c* axes, respectively. The crystal structure is maintained by N−H . . . N and N−H . . . S hydrogen bonds (Table 3). The former interactions are observed for N21−H21 from the pn molecule and N1 as well as N4 atoms from thiocyanate anions and result in a shorter Cu3−Zn1 distance and more compact structure of this part of the chain. There were not detected any similar interactions between N11 ligand and thiocyanate anion, and, consequently, that part of the zigzag exposes a more extended structure. N-H . . . S hydrogen bonds mediate interactions between adjacent chains forming a robust network of hydrogen bonds. They involve rather non-bridging sulfur atoms, and the N21−H21a . . . S3[1−x, 1−y, 2−z] bond is the only exception. This hydrogen bonds pattern is due to significant differences in thiocyanate geometry with adjacent metal ions. The detailed analysis of Zn-N-C angles can be found in Supplementary Materials.

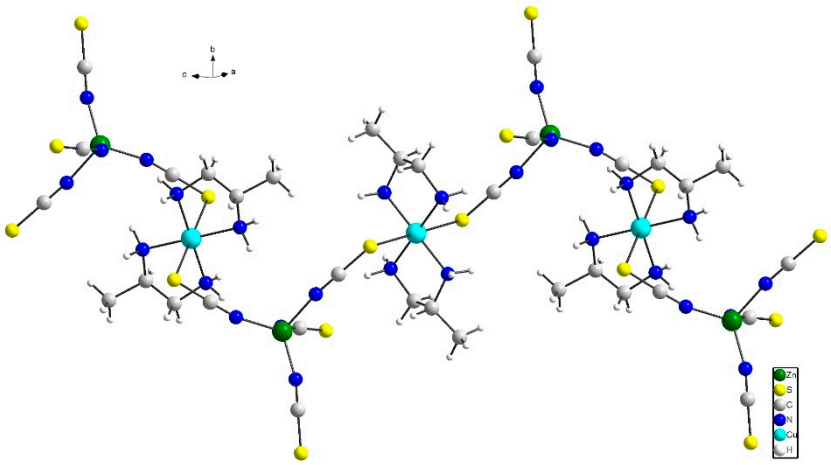

Figure 2. Structure of the chain in **1** viewed along the [1 0 −1] direction.

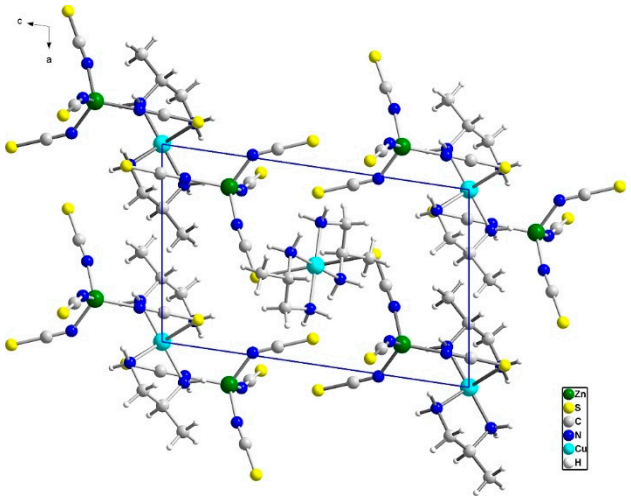

Figure 3. Crystal packing of **1** along the *b*-axis.

Table 3. Hydrogen bonds for **1**.

D-H	A	*d*(D-H) [Å]	*d*(H···A) [Å]	*d*(D···A) [Å]	<DHA [°]
N11-H11A	S2 [1+x,1+y,z]	0.990	2.85	3.696(3)	144
N14-H14A	S1 [–x,1–y,1–z]	0.990	2.46	3.431(3)	167
N21-H21A	N1 [–x,1–y,2–z]	0.990	2.51	3.283(4)	134
N21-H21A	N4 [–x,1–y,2–z]	0.990	2.50	3.365(5)	146
N21-H21B	S3 [1–x,1–y,2–z]	0.990	2.62	3.514(3)	151
N24-N24B	S2 [x,1+y,z]	0.990	2.54	3.446(3)	152

3.2.2. Structure of Compound 2

Compound **2** crystallizes in the monoclinic centrosymmetric *P* $2_1/m$ space group with copper positioned at the inversion center and zinc and two (S1 and S2) thiocyanates located at the *m* plane. In the asymmetric unit of the unit cell, a copper unit was found with only one symmetrically independent *N*,*N*-Me_2-en molecule and a zinc block with three thiocyanate anions (Figure 4). In this structure, *N*,*N*-Me_2-en reveals a positional disorder for CH_2 and CH_3 groups with two populations: 0.62:0.38. The selected bond distances and angles are listed in Table 4 and Table S2. Both copper coordination spheres are composed of four nitrogen atoms from two *N*,*N*-Me_2-en molecules and two sulfur atoms from two thiocyanate anions. Hence, copper(II) ion adopt 4 + 2 coordination with four short Cu−N bonds ranging from 1.980(2) to 2.085(2) Å and two sulfur atoms from thiocyanate anions found at very long identical distances 3.3477(14) Å that can be considered only as a semi-coordination. The N−Cu−N angles show following values 84.79(9) inside the Cu2 chelate ring, 95.21(9)° for atoms belonging to two different organic ligands, and 180.0° for *trans* oriented nitrogen atoms. Sulfur atoms form S−Cu−N angles ranging from 86.86(7) to 93.14(7)°. The zinc(II) ion was found in the tetrahedral environment with four nitrogen atoms from thiocyanate anions forming the coordination sphere. Zn−N bonds are slightly shorter for nitrogen atoms from bridging thiocyanates (1.950(3) Å), whereas, for nitrogen atoms from both non-bridging ligands, we found 1.955(4) and 1.967(4) Å. The N−Zn−N angles range from 108.22(9) to 109.81(10)° for angles between bridging and terminal thiocyanato ligands showing values close to the ideal tetrahedral environment, whereas the angles between the non-bridging ligands (103.70(17)°) as well as between the bridging ligands (116.30(15)°) adopt extreme values for this structure. All thiocyanato ligands were found in linear conformation with an N−C−S angle being close to 180°. The Zn−N−C angle for the bridging thiocyanate (171.9(3)°) falls into the range of terminal ligands: 161.2(4) and 178.2(4)° for N1 and N2 thiocyanates, respectively. The detailed analysis of Cu(II) and Zn(II) coordination spheres for **1**, **2**, and comparison with $Cu(en)_2[Cd(SCN)_3]_2$ [4], $\{Cu(en)_2[Ni(en)(NCS)_2(SCN)]_2\}_n$ [10], $[Cu(en)_2Zn(NCS)_4]\cdot H_2O$ [19], $[Cu(en)_2(SCN)_2]$ [44] and $[Cu(en)_2Cd(dca)_2(SCN)_2]_n$ [45] can be found in Supplementary Materials.

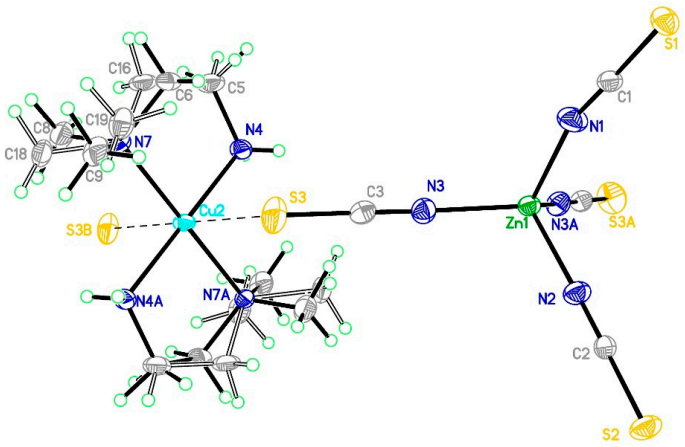

Figure 4. The representative portion of the crystal structure of **2** with the numbering scheme and the thermal ellipsoids at 20% probability.

Table 4. Selected bonds lengths [Å] for **2**.

Bond	Length	Bond	Length
Zn1−N3	1.950(3)	Cu2−N4	1.980(2)
Zn1−N3 [i]	1.950(3)	Cu2−N4 [ii]	1.980(2)
Zn1−N1	1.955(4)	Cu2−N7 [ii]	2.085(2)
Zn1−N2	1.967(4)	Cu2−N7	2.085(2)
		Cu2−S3 [ii]	3.3477(14)
		Cu2−S3	3.3477(14)

[i] x, −y−1/2, z; [ii] −x, −y, −z+1.

In packing, we observe chains running along the *b*-axis showing a regular zigzag pattern with copper(II) ions indicating the axis of this zigzag and zinc(II) cations positioned above and below it (Figures 5 and 6). There is one intermetallic value describing separation between copper and zinc ions in the chain being 6.879 Å, whereas distances between adjacent copper cations and adjacent zinc cations are much bigger, being 8.249 and 13.758 Å, respectively. The Cu2−S3−Zn1 angle is 116.31°. The shortest distances between paramagnetic copper ions are 8.249 and 8.263 Å. The former corresponds to intrachain separation, and it is a half of the *b*-axis, whereas the latter describes a distance between copper(II) ions from two adjacent chains translated along the *a*-axis. The crystal network is maintained via few hydrogen bonds created by sulfur atoms (Table 5). An intrachain hydrogen bond was detected between H9A from the main population of the CH_3 group and a bridging S3 sulfur atom. Additionally, there are two N−H ... S hydrogen bonds between adjacent chains. Hence, NH_2 group is crucial for crystal network formation.

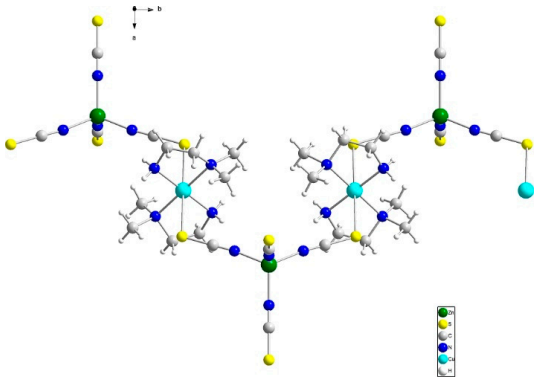

Figure 5. Structure of the chain in **2** viewed along the *b*-axis.

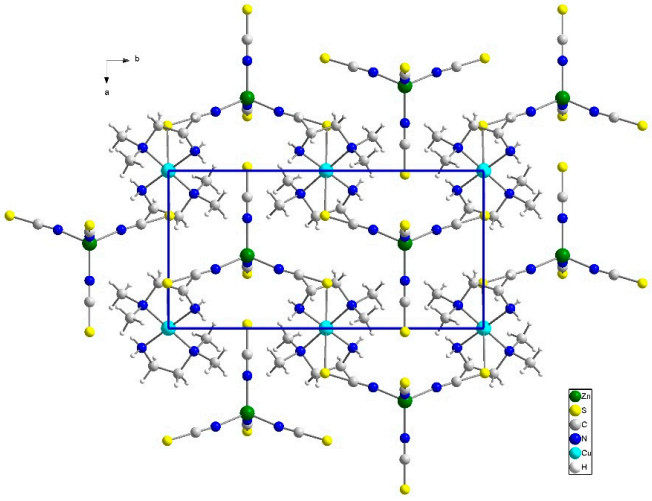

Figure 6. Crystal packing of **2** along the *c*-axis.

Table 5. Hydrogen bonds for **2**.

D-H	A	*d*(D-H) [Å]	*d*(H···A) [Å]	*d*(D···A) [Å]	<DHA [°]
N4-H4A	S2 [x,y,–1+z]	0.822(15)	2.778(13)	3.532(3)	153.2(13)
N4-H4B	S1 [–1+x,y,–1+z]	0.821(14)	2.767(14)	3.485(2)	147.0(13)
C9-H9A	S3 [x,y,z]	0.96	2.66	3.505(8)	147

3.2.3. Structure of Compound 3

The crystal structure of the compound **3** is unknown (see Experimental and Supplementary Materials).

3.3. EPR and Magnetism of 1 and 2

3.3.1. EPR

The compounds **1** and **2** exhibit an axial type of EPR spectra. The room temperature EPR spectra are shown in Figure 7 (for **3,** see Figure S1). This category of spectra is consistent with copper(II) complex of axial "effective symmetry" of ligand field in line with the pseudooctahedral environment [33]. The EPR spectra were simulated using the program SPIN written by Dr. Andrew Ozarowski from NHMFL, University of Florida, with the resonance field calculated by full diagonalization of an energy matrix. A large anisotropy of the line width had to be used in the simulation procedure in the case of **1**. The line width for **2** is ca. 2.5 to 5 times smaller than that for **1** for perpendicular and parallel orientation, respectively (compare Figure 7b with Figure 7a). The simulated g-values, 2.190 (**1**) and 2.195 (**2**) for $g_{\|}$, and 2.054 (**1**) and 2.046 (**2**) for $g_{\perp}$, respectively, correspond to $d_{x^2-y^2}$ ground state of copper(II) ion. According to the perturbation theory, using only the first-order terms in the formulas for $g_{\|}$ and $g_{\perp}$, the G value defined as $G = (g_{\|} - 2) / (g_{\perp} - 2)$ for the $d_{x^2-y^2}$ ground state should be about 4 [33,46]. In our case, those values are 3.5–4.2. Hence, the observed crystal g values are valid and equal to the molecular **g** values describing the symmetry of single paramagnetic center, while the exchange coupling is small but not insignificant (see below) [46].

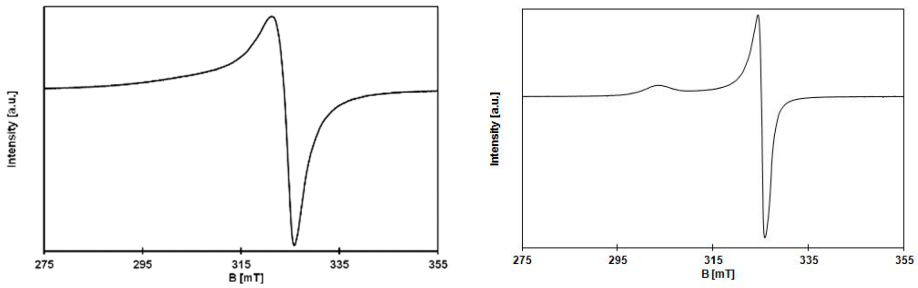

Figure 7. EPR spectra of: (**a**) **1**; (**b**) **2**. Some experimental conditions: powdered samples, room temperature, X-band (9.32364 and 9.32397 GHz for **1** and **2**, respectively).

3.3.2. Magnetism

Magnetic properties of the complexes **1** and **2** were determined in the range 1.8–300 K. The plots of χT are given in Figures 8 and 9 (for **3,** see Figure S2). The values of χT at 300 K are equal 0.414 (**1**) and 0.473 (**2**) $cm^3 \cdot mol^{-1} \cdot K$ with effective magnetic moments 1.82 (**1**) and 1.95 (**2**) B.M. per Cu(II) center, and these are values expected for an single copper(II) ion [47]. As the temperature is decreased, the χT product remains almost unchanged until 50–100 K, and thereafter gradually changes and reaches 0.426 (**1**) and 0.283 (**2**) $cm^3 \cdot mol^{-1} \cdot K$ (1.85 and 1.51 B.M., respectively) at 1.8 K. The slight increase of the value χT for **1** in the low-temperature, i.e., below 20 K, the range may point to the occurrence of very weak ferromagnetic interactions between Cu(II) ions in the crystal network. However, for **2,** the

decrease of the value χT in the low-temperature range is observed. This effect is very pronounced and may manifest occurrence of weak antiferromagnetic interactions between Cu(II) ions.

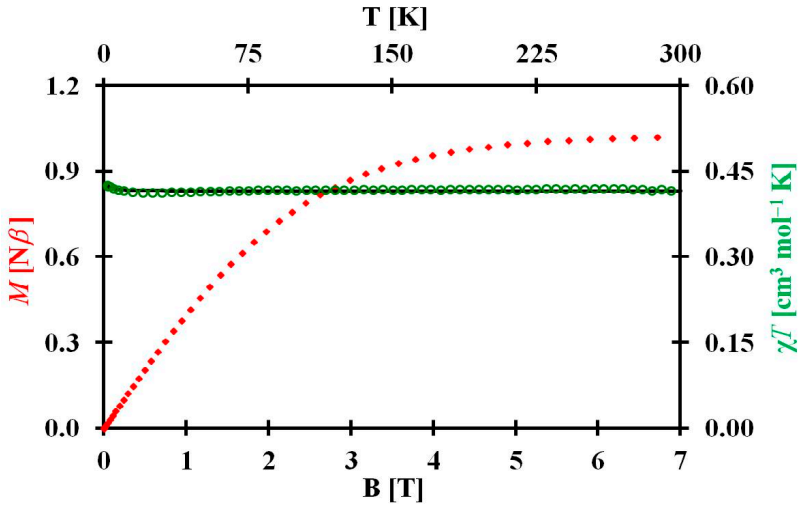

Figure 8. Magnetic properties of **1**: $\chi T(T)$ (**green circles**) at H_{dc} = 1 kOe and $M(\mu_0 H)$ (**red diamonds**) at T = 1.8 K. The solid black line is the best fit for $\chi T(T)$ to the Curie–Weiss model.

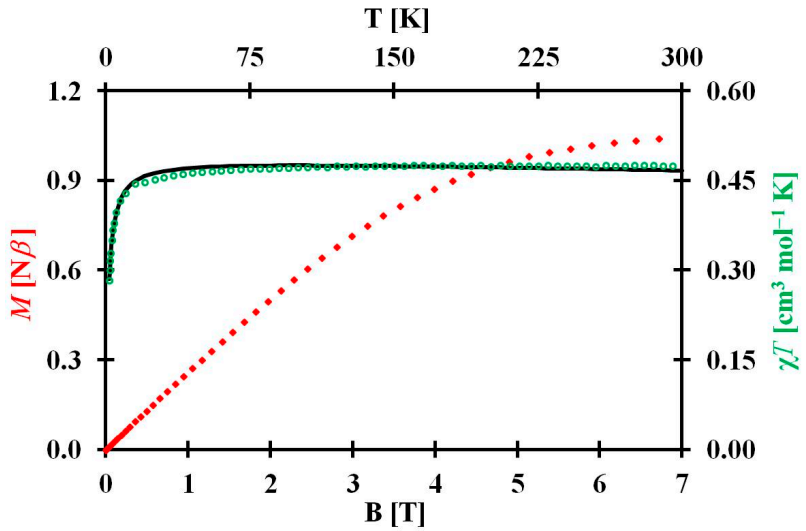

Figure 9. Magnetic properties of **2**: $\chi T(T)$ (**green circles**) at H_{dc} = 1 kOe and $M(\mu_0 H)$ (**red diamonds**) at T = 1.8 K. The solid black line is the best fit for $\chi T(T)$ to the Curie–Weiss model.

The variation of magnetizations (M) versus the magnetic field (B) has been measured at 1.8 K and indicates a linear relation to c.a. 1.0 and 2.4 T for **1** and **2**, respectively. Then, magnetizations continue the Brillouin function (Figures 8 and 9; for **3,** see Figure S2). Values of magnetizations of 1.02 and 1.05 B.M. at 7 T, for **1** and **2**, respectively, confirm the presence of S = 1/2.

3.4. Modelling of Magnetic Interactions

The compounds **1** and **2** investigated in this work form an infinite chains of alternating paramagnetic copper(II) and diamagnetic zinc(II) ions connected by thiocyanato anions forming a pattern –SCN–Zn–NCS–Cu–. In such a case with paramagnetic centers separated by eight bonds and

at least 8.2 Å, we can expect rather weak interactions. Despite this, in order to describe the magnetic properties, we can try to use a Heisenberg–Dirac–Van Vleck Hamiltonian (HDVV) (Equation (1)):

$$\hat{H} = -2J\sum_{i} \hat{S}_i\hat{S}_{i+1}, \quad (1)$$

where J is the exchange parameter, and S is the spin operator. The behavior of a coupled chain of quantum spins with $S = \frac{1}{2}$ was calculated based on classical Fisher [48], and Boner and Fisher papers [49], and a polynomial approximation given by Hiller et al. [50] (Equation (2)):

$$\chi_M = (Ng^2\mu_B{}^2/kT)\,[A + Bx^2]\,[1 + Cx + Dx^3]^{-1}, \quad (2)$$

where $x = |J|/kT$ and A = 0.25000, B = 0.18297, C = 1.5467, D = 3.4443 for $S = \frac{1}{2}$, and the other symbols have their usual meaning. Least-squares fitting of experimental data for **1** and **2** to Equation (2) gives the $2J$, g, and R values collected in Table 6 (R is the factor defined as (Equation 3):

$$R = \Sigma[(\chi)_{exp} - (\chi)_{calc}]^2 / \Sigma(\chi)_{exp}{}^2. \quad (3)$$

Table 6. Magnetic data for $[Cu(diamine)_2Zn(NCS)_4]\cdot nH_2O$ compounds.

Model	HDVV			Curie–Weiss and Molecular Field				
Compound	$2J$	g	$R\cdot10^6$	C	θ [K]	G	zJ'	$R\cdot10^6$
	[cm^{-1}]			[$cm^3\ mol^{-1}\ K$]			[cm^{-1}]	
1	0.040	2.103	8.02	0.415	0.05	2.104	0.063	7.97
2	−1.054	2.261	2.99	0.478 [b]	−1.40 [b]	2.259	−2.011	1.92
[a]	−0.222	2.164	1.70	0.439	−0.24	2.163	−0.331	1.58

[a] Data for $[Cu(en)_2][Zn(NCS)_4]\cdot H_2O$ [19], [b] 10–300 K range.

Exchange interactions in **1** and **2** are undeniably very weak. The reasons are as follows. For the elongated octahedral copper(II) complex, the dx^2-y^2 SOMO orbital is not directed to the bridging ligand. Nevertheless, it is very possible that some spin density also exists on the dz^2 orbital of copper(II) ion considering the deformation of coordination sphere from an "ideal" elongated octahedron. As a consequence of these, a very weak magnetic coupling was observed. A similar effect has been previously observed for some thiocyanato bridged compounds, although the bridging units were paramagnetic and with different metal ions, and structures. The following examples are representative: (i) tetrahedral $[Co(NCS)_4]^{2-}$ [51,52], (ii) trigonal bipyramidal $[Mn(NCS)_5]^{3-}$ [53], (iii) elongated octahedral $[Mn(NCS)_4(H_2O)_2]^{2-}$ [54], (iv) slightly elongated octahedral $[Cr(NCS)_4(NH_3)_2]^{3-}$ (Reinecke's anion) [13,39,55,56], and practically octahedral $[Cr(NCS)_6]^{3-}$ [34–38,57].

The molecular field approximation was also applied as an alternation. It seems very rational remembering that the Cu···Cu distances within and between the chains are comparable (Table 7). The hydrogen bonds (Tables 3 and 5) could also transmit magnetic interaction between paramagnetic centers [17,58]. The temperature dependencies of magnetic susceptibilities in the whole measured range for **1** and the above 10 K for **2** obey the Curie–Weiss law (Equation (4)):

$$\chi_M = C / (T-\theta) \text{ with } C = (Ng^2\mu_B{}^2/3k)\,S(S+1). \quad (4)$$

Table 7. Summary of the structure and magnetic properties of [Cu(diamine)$_2$Zn(NCS)$_4$]·Solv. compounds.

Diamine (Solv.)	**pn (1) (None)**	***N*,*N*-Me$_2$-en (2) (None)**	**en (H$_2$O)**	**en ($\frac{1}{2}$H$_2$O)**	**en (MeCN)**
Crystal system	Triclinic	Monoclinic	Orthorhombic	Orthorhombic	Monoclinic
Space group	*P -1*	*P 2$_1$/m*	*C mcm*	*P 2$_1$ 2$_1$ 2$_1$*	*P 2$_1$*
Chain type	"Irregular" zigzag[a]	Zigzag	Zigzag	Helical	Linear
No. of NCS^- bridging ions	2	2	2	2	1
Cu–S [Å]	Cu2 2.9718 Cu3 3.0432	3.3477	3.0336	2.921 3.218	3.202 3.232
Cu–N [Å]	Cu2 1.993	1.980	2.022	1.99	1.918
	Cu2 2.031	2.085		1.99	1.990
	Cu3 2.006			2.01	2.085
	Cu3 2.017			2.04	2.085
Comment to Cu–N distances	Four pairs of identical (two for each centers)	Two pairs of identical	Four identical	Pair + single + single	Single + single + pair
Copper environment	4 + 2	4 + 2	4 + 2	4 + 1 + 1	4 + 1 + 1 ≈ 4 + 2
Δ in Zn–N [Å]	0.019	0.017	0.280	0.080	0.157
Δ in N–Zn–N [°]	10.45	12.60	14.89	5.30	23.1
Calculated density [Mg/m^3]	1.667	1.587	1.729	1.649	1.627
Cu···Cu [Å] intrachain	8.481	8.249	7.484	9.001 [b]	6.308
Cu···Cu [Å] interchain	7.569 8.663	8.263	8.074 12.414	7.947 [b] 8.651 [b]	9.496 [b] 11.409 [b]
Zn···Zn [Å] intrachain	10.078 12.726	13.758	11.659	8.261 [b]	11.574 [b]
Zn···Zn [Å] interchain	8.663	8.263 11.149	8.074	7.807 [b] 9.120 [b]	6.314 [b] 9.496 [b]
Cu···Zn [Å] intrachain	5.039 6.363	6.872	5.829	5.491 [b] 6.242 [b]	5.783 [b] 5.791 [b]
Cu···Zn [Å] interchain	7.156 7.675	7.011 7.701	7.281	5.780 [b] 6.233 [b]	5.602 [b] 5.629 [b]
Magnetic interaction	Ferro	Antiferro	Antiferro	No data	No data
Reference	This work	This work	[19]	[18]	[18]

[a] Definition—see above p. 3.2.1; [b] Data were calculated on the basis of cif files; they were not given in the original paper [18].

The Weiss constant is defined as Equation (5):

$$\theta = 2S(S + 1)\, zJ' / 3, \quad (5)$$

where J' is the molecular field exchange parameter, and z is the number of the nearest neighbors [59]. The best fitted values of the Curie (C) and Weiss constants (θ), and R factors defined as above are given in Table 6 along with calculated average g and zJ' values. The Curie constant implies the g values that are smaller than average values calculated from EPR spectra. Disagreement between the g values (EPR vs. magnetic susceptibility) are common.

3.5. Comparison of Structures

Structure **1** and Structure **2** copper(II) ions adopt 4 + 2 coordination sphere (distorted octahedron), and a distorted tetrahedral environment of Zn(II) ions occurs in both structures (Table 7). The main difference concerns the topology of the chain in **1** and **2**. For **1,** the "irregular" run of the main chain can be observed, while the chain of the **2** shows the characteristic zigzag shape (Figure 10). These above-mentioned features of the describing complexes are caused by the presence of the crystallographically distinct blocks of Cu ions. In **1,** there are two $[Cu(pn)_2]^{2+}$ moieties, while, in **2,**

there is one $[Cu(N,N\text{-}Me_2\text{-}en)_2]^{2+}$ unit. This difference influences the mutual arrangement and variety of intermetallic distances of the metal ions and ligands along the chain (Table 7). The difference also relates to the localization of zinc ions according to chain direction determined by copper(II) ions. In **1,** angles between the Cu2−Cu3 and Cu2−Zn1 as well as Cu3−Zn1 are 36.3 and 48.3°, respectively, whereas, in **2,** there is only one angle characterizing mutual positions of copper and zinc atoms, and it is much bigger being 53.2° (Scheme 1).

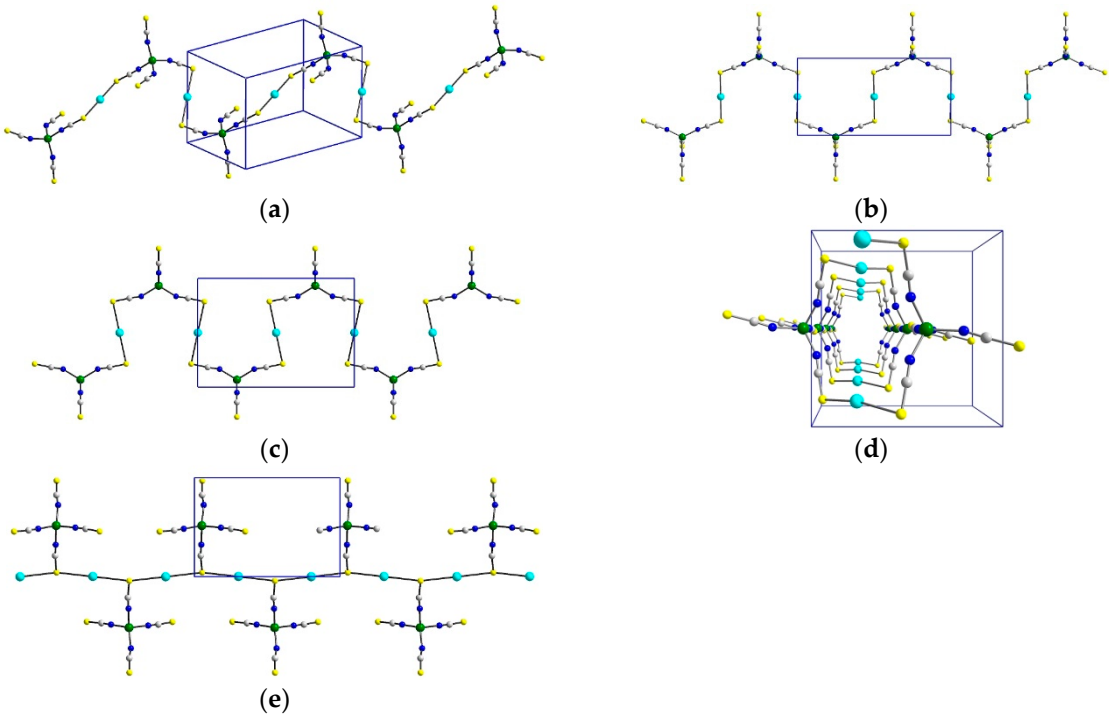

Figure 10. Different chain topologies in $[Cu(diamine)_2Zn(NCS)_4]\cdot$Solv. compounds: (**a**) "irregular" zigzag, **1**; (**b**) zigzag, **2**; (**c**) zigzag, $[Cu(en)_2Zn(NCS)_4]\cdot H_2O$ [19]; (**d**) helical, $[Cu(en)_2Zn(NCS)_4]\cdot\frac{1}{2}H_2O$ [18]; (**e**) linear, $[Cu(en)_2Zn(NCS)_4]\cdot CH_3CN$ [18]. Diamine ligands and solvent molecules are omitted for clarity.

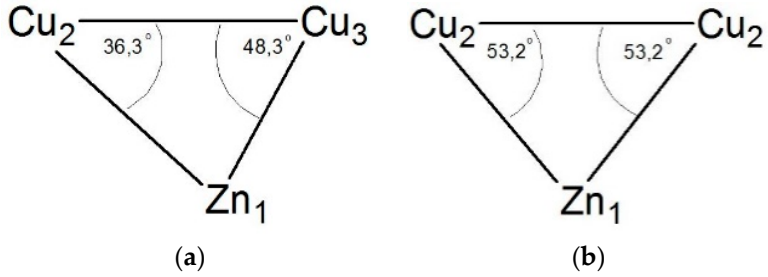

Scheme 1. Mutual arrangement of copper and zinc ions in: (**a**) **1**; (**b**) **2**.

The shortest distances between paramagnetic copper ions are comparable in the both structures and show values as follows: 7.569, 8.481, 8.663 and 8.249, 8.263 Å for **1** and **2**, respectively. The intermetallic value describing separation between copper and zinc ions in the chain of **2** is much longer (6.879 Å) than the Cu−Zn distances in **1** (5.0391(5) and 6.3630(6) Å) (Table 7). Furthermore, the difference in the presence of the crystallographically distinct Cu blocks has an influence on the angles of the coordination sphere of Cu and Zn atoms. In the case of **1,** the C−S−Cu angles directly bonded with the irregular line of the chain are as follows: C3−S3−Cu2 with value 110.38(12) and C4−S4−Cu3 with value 85.00(11). For the C−S−Cu angles in **2,** there is one value 113.30(12). In **1** as well as in **2,** the S−Cu−S angles are 180.0, which indicate the *trans* positions of the S atoms in Cu blocks. In **1,** there is bigger discrepancy for angles included in coordination sphere of Zn, while, in **2,** the range of the values

of N-Zn-N angles (with one except: the angle N3−Zn1−N3^{i}) is more similar (Tables S1 and S2). The occurrence of N−H···N beside the N−H···S hydrogen bond in **1** has the influence on the more compact structure of this part of the chain where they are located, whereas the extended structure is observed if they are missing. This feature does not exist in the case of **2** with only N−H···S hydrogen bonds detected. Furthermore, the non-bridging sulfur atoms in **1** play an important role in maintaining the crystal structure. The same situation takes place in the previously described compound in [19].

The previously described compounds, which show solvatomorphism with the formula $[Cu(en)_2Zn(NCS)_4]\cdot\frac{1}{2}H_2O$ and $[Cu(en)_2Zn(NCS)_4]\cdot$MeCN [18] as well as $[Cu(en)_2Zn(NCS)_4]\cdot H_2O$ [19], are also complexes being one-dimensional chains. However, they show different chain topology (Table 7 and Figure 10). As it was observed in **2**, in $[Cu(en)_2Zn(NCS)_4]\cdot H_2O$, a regular zigzag pattern occurred with a single Cu-Zn distance characterizing the intermetallic separation in the chain. Relatively similar metal arrangement with a zigzag pattern was observed in **1,** but the crucial difference relied on two copper units introducing some irregularities with compressed and extended parts of the chain. The structure containing half of the water molecule adopted a helical shape with a turn being 8.269 Å. The helical structure of the coordination polymer affected the Cu-Cu distance with 9.001 Å within the chain compared to shorter distances in zigzags (7.484 in $[Cu(en)_2Zn(NCS)_4]\cdot H_2O$, 8.481 (**1**) and 8.249 Å (**2**)). The shortest Cu-Cu distances (6.308 Å) occurs in a compound with acetonitrile molecule. However, it is related to interactions between copper(II) ions mediated by only S2 atoms—in this compound, the same thiocyanate transfers coupling between both Cu(II) cations. In the case of Zn–Zn distances, the shortest (8.261 Å) occurs in a compound with half of the water molecule, with the largest being 13.758 Å in **2**. It should be noted that, due to zinc positions in zigzags, Zn–Zn interchain distances are usually much shorter than intrachain ones except for a helical structure presenting substantially different metal unit arrangement. This compound has the longest Cu-S bond among the compared complexes. This significant elongation of the Cu ions binding towards sulfur atoms may result from steric hindrance caused by the presence of two methyl substituents beard by nitrogen atoms of the diamine amino group. An additional methyl group attached to a carbon atom in **1** results in very short Cu-S bonds observed also for unsubstituted en molecules in the helical structure [18] and $[Cu(en)_2Zn(NCS)_4]\cdot H_2O$ [19]. Therefore, it seems that subtle factors such as solvents (its kind and number of molecules) present in the crystal network are even more crucial for Cu-S distances. It is confirmed by a large range of these contacts for en complexes ranging from 2.921 Å to 3.232 Å [18]. On the contrary, Cu-N bonds usually depend on the substituents attached to nitrogen atoms with the longest distances found for **2**, whereas these bonds in pn and en complexes are similar. The helical structure is exceptional because it shows huge asymmetry with very short and very long Cu-N bonds. In the latter case, they are such length as for the unsubstituted ligand as for *N*,*N*-Me_2-en with two nitrogen atoms bearing two methyl groups in **2**.

4. Conclusions

In this paper, we presented three new heterometallic compounds with the formula $[Cu(diamine)_2Zn(NCS)_4]\cdot nH_2O$ (diamine / n = pn / 0; *N*,*N*-Me_2-en, 0; *N*-Me-en, $\frac{1}{2}$) were characterized by elemental analysis, IR, electronic, and EPR spectra, single crystal XRD, and magnetic studies. At least in two cases, 1D chains were detected with thiocyanates acting as bridges. In these cases, Cu-S elongated coordination bonds complete the copper(II) spheres resulting in 4 + 2 coordination. The details of the coordination concerning Cu-S and Cu-N bonds depend on substituent position affecting steric hindrance and hence a topology of the chain revealing different zigzag patterns characterized by one (regular) or two ("irregular") Cu-Zn distance values. Pryma et al. [18] reported two similar chain structures but showing another topology i.e., helical or linear, with different connectivity and/or mutual unit orientations. It proves that even subtle changes of solvent, water molecules numbers, synthesis conditions, and diamine results in the different observed topologies.

Solid state magnetic characterization of $[Cu(diamine)_2Zn(NCS)_4]\cdot nH_2O$ compounds reveals a ferromagnetic (pn) vs. antiferromagnetic (*N*,*N*-Me_2-en) interactions between paramagnetic copper(II)

metal centers. Presumably, the used diamine ligand, shape of the zigzag chain, and hydrogen interactions have the influence on the occurrence and type of magnetic interaction in obtained compounds. Both approaches of treatment of magnetic data, i.e., one-dimensional chain (HDVV) and simple Curie–Weiss models, give similar results (Table 6), which suggests that the interactions through thiocyanato bridges are negligible or comparable with interactions through hydrogen bonds. This is not strange, considering the structural aspects discussed above. Missing magnetic data for structures reported by Pryma et al. [18] impede any magnetostructural correlations.

Supplementary Materials: The following are available online at http://www.mdpi.com/2073-4352/9/12/637/s1, Comparison of coordination spheres in 1 and 2 with literature data, Discussion of NCS and Zn-N-C angles, Table S1: Selected bond lengths [Å] and angles [°] for **1,** Table S2: Selected bond lengths [Å] and angles [°] for **2**, Structure of compound **3, Figure S1**: EPR spectrum of **3**, Figure S2: Magnetic properties of **3**, References.

Author Contributions: Conceptualization, N.T. and G.W.; Formal analysis, N.T., T.M.M., and G.W.; Investigation, N.T., T.M.M., R.P., and G.W.; supervision, G.W.; Writing—original draft, N.T., T.M.M., and G.W.; Writing—review and editing, R.P. and G.W.

Funding: This research was funded by the Ministry of Science and Higher Education, Republic of Poland (Core funding for statutory R & D activities). N.T. thanks Faculty of Chemistry Nicolaus Copernicus University for financial support (Grants for Young Scientist, No. 2074-Ch). Magnetic measurements were performed using the equipment purchased from the Large Research Infrastructure Fund of the Polish Ministry of Science and Higher Education (decision No. 6350/IA/158/2013.1).

Acknowledgments: Diffraction data were collected on BL14.2 at the BESSY II electron storage ring operated by the Helmholtz–Zentrum Berlin [60]. We would particularly like to acknowledge the help and support of Piotr Wilk during the experiment.

Conflicts of Interest: The authors declare no conflict of interest. The funders had no role in the design of the study; in the collection, analyses, or interpretation of data; in the writing of the manuscript, or in the decision to publish the results.

References and Note

1. Burmeister, J.L. Ambidentate ligands, the schizophrenics of coordination chemistry. *Coord. Chem. Rev.* **1990**, *105*, 77–133. [CrossRef]
2. Kabešová, M.; Boča, R.; Melník, M.; Valigura, D.; Dunaj-Jurčo, M. Bonding properties of thiocyanate groups in copper (II) and copper (I) complexes. *Coord. Chem. Rev.* **1995**, *140*, 115–135. [CrossRef]
3. Housecroft, C.E.; Sharpe, A.G. *Inorganic Chemistry*, 4th ed.; Pearson Education Limited: Harlow, UK, 2012; pp. 655, 824, 993.
4. Shen, L.; Feng, X. Synthesis and Crystal Structure of a Novel Polymeric Thiocyanato-Bridged Heteronuclear Complex of Copper (II) and Cadmium (II). *Struct. Chem.* **2002**, *13*, 437–441. [CrossRef]
5. Mroziński, J.; Kłak, J.; Kruszyński, R. Crystal structure and magnetic properties of the 1D bimetallic thiocyanate bridged compound: {(CuL_1)[$Co(NCS)_4$]}(L_1 = *N-rac*-5,12-Me_2-[14]-4,11-dieneN_4). *Polyhedron* **2008**, *27*, 1401–1407. [CrossRef]
6. Skorupa, A.; Korybut-Daszkiewicz, B.; Mroziński, J. Heteronuclear thiocyanate-bridged compounds of the type $(NiL)_3[M(NCS)_6]_2$ (M = Fe(III), Cr(III); L = 5,6,12,13-Me_4-[14]-4,11-dieneN_4). *Inorg. Chim. Acta* **2002**, *336*, 65–70. [CrossRef]
7. Skorupa, A.; Korybut-Daszkiewicz, B.; Mroziński, J. Crystal structure and magnetic properties of two heteronuclear thiocyanate bridged compounds: (CuL)[$Co(NCS)_4$] (L = *N-meso*-(5,12-Me_2-7,14-Et_2-[14]-4,11-dieneN_4) and *N-rac*-(5,12-Me_2-7,14-Et_2-[14]-4,11-dieneN_4)). *Inorg. Chim. Acta* **2001**, *324*, 286–292. [CrossRef]
8. Wrzeszcz, G.; Dobrzańska, L.; Grodzicki, A.; Wojtczak, A. Magnetostructural characterisation of the first bimetallic assemblies derived from the anionic building block $[Cr(NCS)_6]^{3-}$, $[M(en)_3]_n[\{M(en)_2$-μ-SCN-Cr$(NCS)_4$-μ-NCS$\}_{2n}]$ with M = Ni(II), Zn(II). *J. Chem. Soc. Dalton Trans.* **2002**, 2862–2867. [CrossRef]
9. Nesterova, O.V.; Petrusenko, S.R.; Kokozay, V.N.; Skelton, B.W.; Jezierska, J.; Linert, W.; Ozarowski, A. Structural, magnetic, high-frequency and high-field EPR investigation of double-stranded heterometallic $[\{Ni(en)_2\}_2(\mu\text{-}NCS)_4Cd(NCS)_2]_n \cdot nCH_3CN$ polymer self-assembled from cadmium oxide, nickel thiocyanate and ethylenediamine. *Dalton Trans.* **2008**, 1431–1436. [CrossRef]

10. Shen, L.; Xu, Y.-Z. Structure and magnetic properties of a novel two-dimensional thiocyanato-bridged heterometallic polymer $\{Cu(en)_2[Ni(en)(SCN)_3]_2\}_n$. *J. Chem. Soc. Dalton Trans.* **2001**, 3413–3414. [CrossRef]
11. Krautscheid, H.; Emig, N.; Klaassen, N.; Seringer, P. Thiocyanato complexes of the coinage metals: Synthesis and crystal structures of the polymeric pyridine complexes $[Ag_xCu_y(SCN)_{x+y}(py)_z]$. *J. Chem. Soc. Dalton Trans.* **1998**, 3071–3077. [CrossRef]
12. Machura, B.; Świtlicka, A.; Zwoliński, P.; Mroziński, J.; Kalińska, B.; Kruszynski, R. Novel bimetallic thiocyanate-bridged Cu(II)–Hg(II) compounds—Synthesis, X-Ray studiem and magnetic properties. *J. Solid State Chem.* **2013**, *197*, 218–227. [CrossRef]
13. Nikitina, V.M.; Nesterova, O.V.; Kokozay, V.N.; Zubatyuk, R.I.; Dyakonenko, V.V.; Shishkin, O.V.; Goreshnik, E.A.; Gómez-García, C.J.; Clemente-Juan, J.M.; Jezierska, J. Supramolecular diversity and magnetic properties of novel heterometallic Cu(II)/Cr(III) complexes prepared from copper powder, Reineckes salt and ethylenediamine. *Inorg. Chim. Acta* **2009**, *362*, 2237–2246. [CrossRef]
14. Kobayashi, M.; Savard, D.; Geisheimer, A.R.; Sakai, K.; Leznoff, D.B. Heterobimetallic Coordination Polymers Based on the $[Pt(SCN)_4]^{2-}$ and $[Pt(SeCN)_4]^{2-}$ Building Blocks. *Inorg. Chem.* **2013**, *52*, 4842–4852. [CrossRef] [PubMed]
15. Mousavi, M.; Béreau, V.; Desplanches, C.; Duhayon, C.; Sutter, J.-P. Substantial exchange coupling for {Mo–NCS–M} combination: Illustration for 1-D $[\{Mo(NCS)_6\}\{NiL\}_2(NCS)]_n$. *Chem. Commun.* **2010**, *46*, 7519–7521. [CrossRef] [PubMed]
16. Khandar, A.A.; Klein, A.; Bakhtiari, A.; Mahjoub, A.R.; Pohl, R.W.H. One-dimensional ladder like and two-dimensional polymorphs of heterometallic thiocyanate bridged copper (II) and mercury (II) coordination polymer: Syntheses, structural, vibration, luminescence and EPR studies. *Inorg. Chim. Acta* **2011**, *366*, 184–190. [CrossRef]
17. Tercero, J.; Diaz, C.; Ribas, J.; Ruiz, E.; Mahía, J.; Maestro, M. New Oxamidato-Bridged CuII-NiII Complexes: Supramolecular Structures with Thiocyanate Ligands and Hydrogen Bonds. Magnetostructural Studies: DFT Calculations. *Inorg. Chem.* **2002**, *41*, 6780–6789. [CrossRef]
18. Pryma, O.V.; Petrusenko, S.R.; Kokozay, V.N.; Skelton, B.W.; Shishkin, O.V.; Teplytska, T.S. A Facile Direct Synthesis of Bimetallic $Cu^{II}Zn^{II}$ Complexes with Ethylenediamine Revealing Different Types of Chain Crystal Structures. *Eur. J. Inorg. Chem.* **2003**, 1426–1432. [CrossRef]
19. Wrzeszcz, G.; Muzioł, T.M.; Tereba, N. Synthesis, characterization and crystal structure of a 1D thiocyanato bridged $[Cu(en)_2Zn(NCS)_4]\cdot H_2O$. Comparison of the three structures with the same $[Cu(en)_2Zn(NCS)_4]$ unit—Different in structural terms. *J. Mol. Struct.* **2015**, *1083*, 374–380. [CrossRef]
20. Wrzeszcz, G.; Muzioł, T.M.; Tereba, N. Corrigendum to Synthesis, characterization and crystal structure of a 1D thiocyanato bridged $[Cu(en)_2Zn(NCS)_4]\cdot H_2O$. Comparison of the three structures with the same $[Cu(en)_2Zn(NCS)_4]$ unit—Different in structural terms [J. Mol. Struct. 1083 (2015) 374–380]. *J. Mol. Struct.* **2015**, *1091*, 236. [CrossRef]
21. Legendre, A.O.; Mauro, A.E.; Ferreira, J.G.; Ananias, S.R.; Santos, R.H.A.; Netto, A.V.G. A 2D coordination polymer with brick-wall network topology based on the $[Cu(NCS)_2(pn)]$ monomer. *Inorg. Chem. Commun.* **2007**, *10*, 815–820. [CrossRef]
22. You, Z.-L.; Ng, S.W. (1,3-Propanediamine-κ^2N,N')bis(thiocyanato-κN)copper(II). *Acta Crystallogr. Sect. E Struct. Rep. Online* **2007**, *63*, m2347. [CrossRef]
23. Bain, G.A.; Berry, J.F. Diamagnetic Corrections and Pascal's Constants. *J. Chem. Educ.* **2008**, *85*, 532–536. [CrossRef]
24. Boča, R. Magnetic Parameters and Magnetic Functions in Mononuclear Complexes Beyond the Spin-Hamiltonian Formalism. In *Structure and Bonding*; Mingos, D.M.P., Ed.; Springer: Berlin, Germany, 2006; Volume 117, pp. 1–264. [CrossRef]
25. *CrysAlis RED and CrysAlis CCD*; Oxford Diffraction Ltd.: Abingdon, UK, 2000.
26. Sheldrick, G.M. A short history of *SHELX*. *Acta Crystallogr. Sect. A Found. Adv.* **2008**, *64*, 112–122. [CrossRef] [PubMed]
27. Brandenburg, K. *DIAMOND, Release 2.1e*; Crystal Impact GbR: Bonn, Germany, 2001.
28. Farrugia, L.J. ORTEP-3 for Windows-a version of ORTEP-III with a Graphical User Interface (GUI). *J. Appl. Crystallogr.* **1997**, *30*, 565. [CrossRef]
29. Sheldrick, G.M. Crystal structure refinement with SHELXL. *Acta Crystallogr. Sect. C Struct. Chem.* **2015**, *71*, 3–8. [CrossRef]

30. www.ccdc.cam.ac.uk.data_request/cif.
31. Lever, A.B.P. *Inorganic Electronic Spectroscopy*, 2nd ed.; Elsevier: Amsterdam, The Netherlands, 1984; pp. 554–572.
32. Procter, I.M.; Hathaway, B.J.; Nicholls, P. The Electronic Properties and Stereochemistry of the Copper (II) Ion. Part I. Bis(ethylenediamine)copper(II) Complexes. *J. Chem. Soc. A* **1968**, 1678–1684. [CrossRef]
33. Hathaway, B.J.; Billing, D.E. The electronic properties and stereochemistry of mono-nuclear complexes of the copper (II) ion. *Coord. Chem. Rev.* **1970**, *5*, 143–207. [CrossRef]
34. Dobrzańska, L.; Wrzeszcz, G.; Grodzicki, A.; Rozpłoch, F. Synthesis and Characterization of Thiocyanato-Bridged Heteropolynuclear Chromium (III)–Copper (II) Complexes. *Polish J. Chem.* **2000**, *74*, 199–206.
35. Dobrzańska, L.; Wrzeszcz, G.; Grodzicki, A.; Rozpłoch, F. Synthesis, Spectroscopy and Magnetism of New μ-Thiocyanato Polynuclear Copper (II)–Chromium (III) Complexes. *Polish J. Chem.* **2001**, *75*, 1689–1694.
36. Wrzeszcz, G.; Dobrzańska, L.; Grodzicki, A.; Rozpłoch, F. Synthesis and Characterization of New Thiocyanato Bridged Complexes with the General Formula $[ML_n]_3[Cr(NCS)_6]_2 \cdot mH_2O$, where M = Cu(II), Ni(II), Co(II); L = Various Substituted Imidazoles. *Polish J. Chem.* **2003**, *77*, 147–156.
37. Wrzeszcz, G. Synthesis and Characterization of New Thiocyanato Bridged Heterobimetallic Complexes with the General Formula: $[Cu(diamine)_2]_3[Cr(NCS)_6]_2 \cdot nH_2O$. *Polish J. Chem.* **2003**, *77*, 845–854.
38. Wrzeszcz, G.; Dobrzańska, L. Magnetic and Thermal Properties of New Thiocyanato Bridged Complexes of the Type $[M(diamine)_2]_3[Cr(NCS)_6]_2 \cdot nH_2O$, where M = Cu(II), Ni(II). *Polish J. Chem.* **2003**, *77*, 1245–1254.
39. Wrzeszcz, G.; Grzebielucha, T. Synthesis and Properties of New Bimetallic Complexes of General Formula: $[Cu(diamine)_2][Cr(NCS)_4(NH_3)_2]_2$. *Polish J. Chem.* **2009**, *83*, 1575–1582.
40. Nakamoto, K. *Infrared and Raman Spectra of Inorganic and Coordination Compounds*, 6th ed.; John Wiley & Sons, Inc.: Hoboken, NJ, USA, 2009; pp. 120–126.
41. Lever, A.B.P.; Mantovani, E. The Far-Infrared and Electronic Spectra of Some Bis-Ethylenediamine and Related Complexes of Copper (II) and the Relevance of These Data to Tetragonal Distortion and Bond Strengths. *Inorg. Chem.* **1971**, *10*, 817–826. [CrossRef]
42. Forster, D.; Horrocks, W.D., Jr. Vibrational spectra and force constants of $Zn(NCO)_4^{2-}$, $Zn(NCS)_4^{2-}$, and $Zn(NCSe)_4^{2-}$. *Inorg. Chem.* **1967**, *6*, 339–343. [CrossRef]
43. Chattopadhyay, S.; Bhar, K.; Das, S.; Chantrapromma, S.; Fun, H.-K.; Ghosh, B.K. Syntheses, structures and properties of homo- and heterobimetallic complexes of the type $[Zn(tren)NCS]_2[M(NCS)_4]$ [tren = tris(2-aminoethyl)amine; M = Zn, Cu]. *J. Mol. Struct.* **2010**, *967*, 112–118. [CrossRef]
44. Brown, B.W.; Lingafelter, E.C. The Crystal Structure of Bis(ethylenediamine)copper(II) Thiocyanate. *Acta Crystallogr.* **1964**, *17*, 254–259. [CrossRef]
45. Nesterova (Pryma), O.V.; Petrusenko, S.R.; Kokozay, V.N.; Skelton, B.W.; Linert, W. A new 2D heterometallic Cu/Cd mixed-anion polymer with dicyanamide and thiocyanate bridges formed via the reaction of elemental copper, cadmium dicyanamide and ethylenediamine. *Inorg. Chem. Comm.* **2004**, *7*, 450–454. [CrossRef]
46. Hathaway, B.J. The Correlation of the Electronic Properties and Stereochemistry of Mononuclear $\{CuN_{4-6}\}$ Chromophores. *J. Chem. Soc. Dalton Trans.* **1972**, 1196–1199. [CrossRef]
47. Kahn, O. *Molecular Magnetism*; VCH Publishers Inc.: New York, NY, USA, 1993; pp. 10–12.
48. Fisher, M.E. Magnetism in One-Dimensional Systems—The Hesisenberg Model for Infinite Spin. *Am. J. Phys.* **1964**, *32*, 343–346. [CrossRef]
49. Bonner, J.C.; Fisher, M.E. Linear Magnetic Chains with Anisotropic Coupling. *Phys. Rev.* **1964**, *135*, A640–A658. [CrossRef]
50. Hiller, W.; Strähle, J.; Datz, A.; Hanack, M.; Hatfield, W.E.; Ter Haar, L.W.; Gütlich, P. Synthesis, Structure, and Magnetic Properties of catena-(μ-Oxo)(hemiporphyrazinato)iron(IV), the First Polymeric μ-Oxo-Bridged Complex of Iron. *J. Am. Chem. Soc.* **1984**, *106*, 329–335. [CrossRef]
51. Francese, G.; Ferlay, S.; Schmalle, H.W.; Decurtins, S. A New 1D bimetal lic thiocyanate-bridged copper (II)-cobalt(II) compound. *New J. Chem.* **1999**, *23*, 267–269. [CrossRef]
52. Tomkiewicz, A.; Kłak, J.; Mroziński, J. Bimetallic complexes with macrocyclic ligands. Variation of magnetic exchange interactions in some heteronuclear thiocyanato-bridged compounds. *Mater. Sci. Pol.* **2004**, *22*, 253–263.

53. Quan, Y.-P.; Yin, P.; Han, N.-N.; Yang, A.-H.; Gao, H.-L.; Cui, J.-Z.; Shi, W.; Cheng, P. Novel hetero-polynuclear metal complexes $(CuL)_3[Mn(NCS)_5]_2$ and $(NiL)_3[Mn(NCS)_5]_2$ containing trigonal bipyramidal geometric $[Mn(NCS)_5]^{3-}$ as bridging ligand. *Inorg. Chem. Commun.* **2009**, *12*, 469–472. [CrossRef]
54. Kou, H.-Z.; Liao, D.-Z.; Cheng, P.; Jiang, Z.-H.; Yan, S.-P.; Wang, G.-L.; Yao, X.-K.; Wang, H.-G. A new one-dimensional thiocyanato-bridged bimetallic compound $[Cu(en)_2Mn(NCS)_4(H_2O)_2]_n$. Synthesis, crystal structure, and magnetic properties. *Can. J. Chem.* **1998**, *76*, 1102–1107. [CrossRef]
55. Zhang, K.-L.; Chen, W.; Xu, Y.; Wang, Z.; Zhong, Z.J.; You, X.-Z. Crystal structure and magnetic properties of a thiocyanato-bridged dinuclear Cr (III)-Cu (II) complex $[(HLCu(SCN)Cr(NCS)_3(NH_3)_2]$·DMF. *Polyhedron* **2001**, *20*, 2033–2036. [CrossRef]
56. Nikitina, V.M.; Nesterova, O.V.; Kokozay, V.N.; Goreshnik, E.A.; Jezierska, J. The first heterometallic Cu(II)/Cr(III) complex with an open-chain Schiff-base ligand self-assembled from copper powder, Reineckes salt, ethylenediamine and acetone. *Polyhedron* **2008**, *27*, 2426–2430. [CrossRef]
57. Smékal, Z.; Březina, F.; Šindelář, Z.; Klička, R.; Nádvornik, M. Polynuclear complexes of chromium (III), copper (II) or nickel (II) with thiocyanato as a bridging ligand. *Transition Met. Chem.* **1997**, *22*, 299–301. [CrossRef]
58. Vasková, Z.; Moncol, J.; Korabik, M.; Valigura, D.; Švorec, J.; Lis, T.; Valko, M.; Melník, M. Supramolecular dimer formation through hydrogen bond extensions of carboxylate ligands—Path for magnetic exchange. *Polyhedron* **2010**, *29*, 154–163. [CrossRef]
59. O'Connor, C.J. Magnetochemistry—Advances in Theory and Experimentation. In *Progress in Inorganic Chemistry*; Lippard, S.J., Ed.; John Wiley & Sons, Inc.: New York, NY, USA, 1982; Volume 29, pp. 203–283. [CrossRef]
60. Mueller, U.; Förster, R.; Hellmig, M.; Huschmann, F.U.; Kastner, A.; Malecki, P.; Pühringer, S.; Röwer, M.; Sparta, K.; Steffien, M.; et al. The macromolecular crystallography beamlines at BESSY II of the Helmholtz-Zentrum Berlin: Current status and perspectives. *Eur. Phys. J. Plus* **2015**, *130*, 141. [CrossRef]